IOP Conf. Series: Materials Science and Engineering **152** (2016) 012022 doi:10.1088/1757-899X/152/1/012022

Flight dynamics and control modelling of damaged asymmetric aircraft

T T Ogunwa and E J Abdullah*

Department of Aerospace Engineering, Faculty of Engineering, Universiti Putra Malaysia, Malaysia

*ermira@upm.edu.my

Abstract. This research investigates the use of a Linear Quadratic Regulator (LQR) controller to assist commercial Boeing 747-200 aircraft regains its stability in the event of damage. Damages cause an aircraft to become asymmetric and in the case of damage to a fraction (33%) of its left wing or complete loss of its vertical stabilizer, the loss of stability may lead to a fatal crash. In this study, aircraft models for the two damage scenarios previously mentioned are constructed using stability derivatives. LQR controller is used as a direct adaptive control design technique for the observable and controllable system. Dynamic stability analysis is conducted in the time domain for all systems in this study.

1. Introduction

Since the beginning of flight, aircraft control has been one of the top priorities of the aviation industry to ensure safe flight. Just like the human body, every part of an aircraft plays a role in ensuring the safe flight and its control. Air transportation is undeniably one of the safest means of transportation in recent times. However, on some occasions, accidents or incidents that involve a number of casualties do occur. Mechanical failure or damage to part(s) of the aircraft is the second most common cause of plane crashes after pilot error, accounting for about 22% of all aviation accidents [1]. Other causes of accidents also include sabotage, loss of control (LOC), weather and other human factors. In the early generation, the flight control systems were mechanical, meaning there was a direct connection between the pilot's control from the cockpit and control surfaces. Over the years, the mechanical flight control system has been replaced by the type that allows the pilot to directly control the motion of the aircraft. This digital type of flight control system uses electrical signals and is referred to by the term 'fly-by-wire'. This type of flight control system improves the stability and control of the aircraft, and also the pilot's reaction time to a flight disturbance [2].

Furthermore, in a situation where the aircraft experiences system failure of any sort, it becomes asymmetric and the workload of the pilot increases greatly. Floating trim tabs, engine fan bursts, bird strikes and frozen controls are some examples of failures that can limit the control of an aircraft. Be that as it may, in most cases, when these types of failures occur, only the control surfaces are affected while the lifting surfaces are left intact. The Sioux DC-10 crash is one of the very famous examples of a situation like this. United Airline Flight 232 was flying from Denver to Chicago when the second engine failed and rendered all hydraulic controls useless. The aircraft was then controlled by the two remaining engines and crash landed in Sioux City, Iowa. There were 111 casualties but 185 people survived [3]. This clearly demonstrates the ability of an aircraft to be controlled without the standard control surfaces. In 2003, DHL's Airbus A300B4 suffered surface-to-air missile strike to its left wing.

As a result of this, all hydraulics were disabled and thus eliminating the pilots' influence over the control surfaces completely. The pilots crash landed the aircraft after adjusting the throttle commands and moving the fuel to prevent complete drainage of the left wing's fuel storage [4]. Other significant reported accidents resulting from failures are as follows:

- Braniff Airways – Lockheed L-188 – 1968: Structural limits were exceeded in an attempt to recover from an unusual attitude caused by turbulence. This resulted in the right wing and empennage being separated during flight. The crew and passengers all died in the crash [4].
- Flying Boat Inc. Flight 101- Grumman Turbo Mallard – 2005: The aircraft experienced a right wing separation during flight due to fatigue and fracture damage in the right wing. All the passengers on board were killed after the aircraft crashed into a shipping channel [4].
- Piper PA-32 – 2006: Few minutes after a Boeing 737 had taken off, this aircraft was piloted into the same flight path. The aircraft was overstressed by the wake turbulence and it caused a section of the left wing, portions of the right wing's flap, left and right side of the stabilator and aileron to be separated. Only the pilot was killed in the crash [4].

While more examples abound, the scenarios listed above show instances of engine, wing and also control surface damage. Sadly, despite improved maintenance and inspection efforts, accidents still occur. Therefore, it is of utmost importance to develop adaptive methods to recover the aircraft from damage(s).

As it is not practical to consider all possible damage scenarios, the study focuses on two damage situations: 33% loss of the left wing from the tip and complete loss of the vertical stabilizer. In this study, a Linear Quadratic Regulator (LQR) is implemented to aid a damaged Boeing 747-200 aircraft that has a controllable and observable system even after damage in landing safely. LQR controller is an optimal controller and is chosen for this study because it is straightforward and easy to implement or use for multivariable systems, especially with the aid of computer programs. Also, for a full state feedback system, the optimal input signal can be obtained and the control output minimized.

2. Background review

This section gives reviews on past and current studies that have been carried out in the area of control of damaged asymmetric aircraft. In the first sub section, scaled models that have been used to model aircraft damage(s) are discussed. Sub sections two and three highlight studies that have been carried out to see how damage affects the aerodynamics and flight dynamics of an aircraft, respectively. Some adaptive control techniques used in previous studies are discussed in sub section four.

2.1. Scaled models

Loss of control has been a major motivation in the aerospace industry as a whole. A lot of researches have been carried out in a bid to provide solution or resolve cases involving loss of control of aircraft due to damage(s). Subscale model of a commercial aircraft known as AirSTAR was developed by the National Aeronautics and Space Administration(NASA) Langley to investigate events relating to loss of control. Cunningham *et al.* [4] discussed the details of the first subscale aircraft known as S-2 aircraft and its ground facilities. Simply described, the S-2 is an off-the-shelf aircraft model but it is fitted with further instrumentation. The aircraft was used in the development of ground facilities and procedures, allowing for more expensive scaled aircraft to be developed with less risk. The facilities in AirSTAR are able to estimate the aircraft's aerodynamic parameters in real time. This is an important feature because wind tunnel data for the S-2 can be obtained and can be used for the validation of wind tunnel data in the future. Apart from the S-2 aircraft, Jordan *et al.* [5, 6] developed two dynamically scaled aircraft known as GTM-T1 and GTM-T2. These aircraft were scaled to be about 5.5% of size of an actual commercial aircraft but the GTM-T2 was designed to have a lighter airframe so that more instrumentation and electronics could be added. As for the aircraft moments of inertia, they were scaled proportionally with geometric scaling. Also, the weight was slightly increased to make up for the increase in lift as the aircraft fly at lower altitudes, which have higher air density. One can estimate the weight of aircraft parts by comparing the available data for similar aircraft. This method was used

by Beltramo *et al.* [7] to estimate the weights of the components of a commercial aircraft. It was noted that knowing takeoff weight of an aircraft is enough to estimate the weight of its wing.

2.2. Aerodynamics

The effect of the loss of wing tip on the aerodynamic stability derivatives of the aircraft, as well as the static aeroelastic effects, was explored by Woo [8]. In doing that, detailed finite element wing structure model was joined to a doublet lattice model for a fighter jet. The introduction of a rolling moment coefficient due to pitch was noted to be the most significant effect of damage among the investigated damage cases. There was also significant coupling between the pitch and yaw. For the study of the aerodynamic effects of a hole in the wing, Render *et al.* [9] used wing tunnel testing method. It was observed that this type of damage resulted in two patterns: a weak-jet and a strong-jet. In the case of the weak-jet, the flow remained attached and the hole affected the overall aerodynamic loads only a little. For the strong-jet however, the flow did not remain attached to the hole and therefore had more significant effects on the aerodynamic loads. The damage caused the drag to increase greatly for a hole close to the trailing edge and lift to be decreased as the damage progressed forward.

Extensive wind tunnel testing has also been carried out on the Generic Transport Model (GTM) for different loss of control scenarios. Foster *et al.* [10] carried out initial tests for the GTM and focused on aerodynamic properties at very high angles of attack of range -5^{o} to 85^{o} and sideslip angles ranging between -45^{o} to 45^{o}. The basis of these studies uses existing techniques for fighter aircraft and the tests carried out included that of rotary balance, static and forced oscillation. The hysteresis effects on the aerodynamic forces at large angles were observed in the studies. An attempt was made to understand the cause of these effects using flow visualisation but the results came up inconclusive. To take care of the time dependent effects, the aerodynamic forces were averaged. The tests however showed that loss of static stability can be as a result of large angles of attack. In addition, loss of rudder effectiveness at large angles of attack was also observed.

For the exploration of effects of damage on GTM aircraft, Shah [11] conducted more wind tunnel tests recently. The cases investigated include 3 horizontal tail loss cases, 6 wing tip loss cases, 3 cases of horizontal tail loss and other cases like holes in the lifting surfaces. The results of these tests showed that reduction in the lift curve slope due to reduced aspect ratio is eminent if the aircraft experiences the loss of a wing tip. The rolling moment observed by Woo [8] was also observed in these tests. Furthermore, it was noted that trimming the aircraft at negative sideslip can reduce the rolling moment experienced at trim. Rawlings [8] also carried out wind tunnel tests on the GTM to explore how the stabilator can be utilized as a speed break-brake or to recover from the loss of control. The detailed configuration of the GTM was addressed, especially the travel limits for the control surfaces. The tests result showed that there was no benefit in the use of the stabilator for recovery after loss of control but the stabilator was useful for speed brake purposes. Nonetheless, the usefulness of the stabilator was limited because of significant loading.

Thomas [12] used the lifting surface theory to explore the aerodynamics properties of a bird with an asymmetric tail or wing. He observed that the effects of asymmetry include increased turn radius and reduced lift. These effects however were not as pronounced when the asymmetry was in the tail of the bird. Disturbances to the aircraft can bring about significant aerodynamic nonlinearities. The effects of these disturbances were captured by Keller *et al.* [13] using the non-linear line theory. The wake effect was modelled using a code that was previously used for rotorcraft. This model was compared to the flight test data of a small radio-controlled aircraft and the results seemed to correlate.

2.3. Flight dynamics

In a bid to understand what causes the loss of control of an aircraft, Wilborn and Foster [14] defined a set of five quantitative metrics that includes the structural integrity envelope (airspeed and load factor) and the adverse aerodynamic envelope (angle of attack and sideslip). The study was carried out in such a way that if one of these envelopes established was exceeded, it resulted in an upset condition which was sometimes recoverable. As more envelopes were exceeded, the difficulty of recovery would also increased. Also, the aircraft experienced loss of control once three of these limits had been exceeded.

Damage to part of an aircraft causes the centre of gravity to shift and the simulation using cg-centric equations of motion becomes more complicated. Bacon and Gregory [15] succeeded in overcoming this complication by deriving the equations of motion about a fixed point. The equations of motion were then calculated using Newton's method so that the centre of gravity offset is a system parameter. This method allows for discontinuous changes of the centre of gravity's location without causing discontinuities in the system states. Although a new set of equations were employed in this study, the yielded results are equivalent to that of the traditional cg-centric equation method and even has an advantage of being simple to implement. Nguyen *et al.* [16, 17] initially used similar equations but the original equations of motion did not correctly model the change in the centre of gravity and thus were adjusted in a later erratum [18]. In order to account for damage effects, the steady level flight condition was considered as having a non-zero sideslip angle or roll angle. A finite differencing approach was then used to calculate the trim with respect to the trim of the undamaged aircraft. In the development of this model, the linear stability derivatives were obtained from a vortex lattice model of the GTM and were used to get the aerodynamic effects. An adaptive control plan based on dynamic inversion was then implemented in the resulting flight dynamics model. In the end, a recursive least squares or neural network was used to update the baseline dynamic inversion law and to achieve indirect control. To improve the performance of the flight dynamic system, a direct controller was used.

With the aim of a Model Reference Adaptive Controller (MRAC), Liu *et al.* [19] explored the flight dynamics of a damaged aircraft. The focus of this study was geared towards developing a linear model of the aircraft using the same linearized form of equations of motion as Bacon and Gregory [15]. The result showed that, for three input-output cases, the zero dynamics or relative degree were not affected and the system was minimum phased. The sign of the transfer function gain was also not affected. An adaptive controller was then implemented in the model that was able to account for the experienced changes. The effect of the wing tip loss was also investigated by Sarigul-Klijn *et al.* [4], although the stability derivatives of the undamaged aircraft was adjusted by a set of analytical corrections in order to model the loss of wing tip accurately. The reduction in aspect ratio and wing area was focused on in these methods but the coupling introduced had to be for the rolling moment only due to an angle of attack. The equations of motion were derived about a fixed point as with previous studies.

2.4. Adaptive control systems

Without doubt, asymmetric aircraft resulting from structural damage can cause the flight performance and handling quality of the aircraft to deteriorate drastically. Over the years, lots of studies have been carried out to control aircraft during failures. The control of any aircraft begins with identification of the parameters and then adaptive control. Adaptation schemes are therefore implemented directly or indirectly to improve the performance of any control and feedback systems. This study uses the direct adaptive technique where estimation of actual system parameters is avoided and instead will continue to adjust the control laws or even the system controls until the feedback errors are eliminated [20, 21]. What follows is the reviews of prior studies carried out in relation to direct adaptive controls.

Kim and Calise [22] in their work used an adaptive Artificial Neural Network (ANN) as a direct adaptive control for the inverse model of an aircraft. The ANN was modelled offline and coefficients were used to obtain the aircraft dynamics by controlling deflections using sigma-pi neurons and radial basic function. To adapt for errors, an online ANN was also used. The adaptation was actually based on input to the modelled inverse and also the aircraft output. Further research was carried out on the XV-15 Tilt Rotor [23] and involved developing an online training to show the boundedness of the weights of ANNs. The study showed that over a certain range of errors, the adaptive system began to converge to a stable solution. More analysis on bounded weights for various adaptive methods can be found in NASA's Integrated Resilient Aircraft Control (IRAC) in studies carried out by Nguyen, Huang and Bakhtiari-Nejad [21]. Furthermore, from these studies, it was found that for Lyapunov based adaptive law, when high gain occurs, the frequency of oscillations was high and other adaptive methods may be required to get rid of high gain learning.

Model-Reference Adaptive Control System (MRAC) is another direct adaptive control method that can be implemented. Shin *et al.* [24] used dynamic inversion to develop an adaptive output feedback for a modified NASA F-15. In the work they carried out, it was acknowledged that control saturation was possible for both un-adapted and adapted systems. Also, for control and damage rejection, control limitations are based around near saturation deflections. NASA and Boeing conducted simulations and flight tests on various aircraft types, from military to transport. The tests were carried out to show the performance of the flying aircraft using propulsion-only control. Propulsion Controlled Aircraft (PCA) systems tests were carried out on the F-15 and the result showed that the aircraft was able to recover from control failures and upset conditions to eventually land [25]. The PCA flight test was also carried out on the MD-11 and the similar results were achieved. In this case, the aircraft could be controlled manually, as well as make automatic landings [26]. For a Boeing-747, the PCA flight tests showed that aircraft could land successfully after recovering from gust and unusual attitudes [27].

Nguyen *et al.* [17] tested Recursive Least Squares and Lyapunov adaptive laws [21] on a damaged aircraft. The Generic Transport Model (GTM) is modelled in form of a vortex lattice code where the new flight dynamics and aerodynamic coefficient changes are developed and discussed. The new equations of motion for damaged aircraft were also derived at Georgia Tech (GT) [28] and, although the changes in the aerodynamic coefficients were discussed in the GT and NASA papers, the shift in the Center of Gravity(CG) position as a result of damage was excluded. Furthermore, some studies focused on the Flight Control System (FCS) for damaged aircraft. Tang *et al*. [29] used a Proportional Integral Derivative (PID) and an optimal control LQR system to account for the new capabilities and estimated flight envelope of the damaged aircraft, hence directing it towards the safest site to land. The further examination of the aerodynamic coefficients and equations of motion of a damaged aircraft are major contributions of this study.

3. Aircraft models

3.1. Undamaged aircraft model

The Boeing 747-200 aircraft model is used for this study. It is a long range, high capacity, wide body airliner and is the first wide-body aircraft to be built as a freighter, a combination passenger-freighter and a convertible. This aircraft model was chosen for this study primarily due to the fact that the technical specifications, aerodynamics and stability derivatives of the aircraft are widely available. The data for the nominal/undamaged Boeing 747-200 and the flight condition were obtained from [3, 4, 31, 32, 35] and are summarized in Table 1.

For symmetric/undamaged aircraft, linear equations of motion for longitudinal and lateral motions are given by Equations 1 and 2, respectively [30].

$$\begin{bmatrix} \Delta\dot{u} \\ \Delta\dot{w} \\ \Delta\dot{q} \\ \Delta\dot{\theta} \end{bmatrix} = \begin{bmatrix} X_u & X_w & 0 & -g \\ Z_u & Z_w & u_0 & 0 \\ M_u+M_{\dot{w}}Z_u & M_w+M_{\dot{w}}Z_w & M_q+M_{\dot{w}}u_0 & 0 \\ 0 & 0 & 1 & 0 \end{bmatrix} \begin{bmatrix} \Delta u \\ \Delta w \\ \Delta q \\ \Delta\theta \end{bmatrix} + \begin{bmatrix} X_{\delta e} & X_{\delta T} \\ Z_{\delta e} & Z_{\delta T} \\ M_{\delta e}+M_{\dot{w}}Z_{\delta e} & M_{\delta T}+M_{\dot{w}}Z_{\delta T} \\ 0 & 0 \end{bmatrix} \begin{bmatrix} \Delta\delta_e \\ \Delta\delta_T \end{bmatrix} \quad (1)$$

$$\begin{bmatrix} \Delta\dot{\beta} \\ \Delta\dot{p} \\ \Delta\dot{r} \\ \Delta\dot{\phi} \end{bmatrix} = \begin{bmatrix} \frac{Y_\beta}{u_0} & \frac{Y_p}{u_0} & -\left(1-\frac{Y_r}{u_0}\right) & \frac{g\cos\theta_0}{u_0} \\ L_\beta & L_p & L_r & 0 \\ N_\beta & N_p & N_r & 0 \\ 0 & 1 & 0 & 0 \end{bmatrix} \begin{bmatrix} \Delta\beta \\ \Delta p \\ \Delta r \\ \Delta\phi \end{bmatrix} + \begin{bmatrix} 0 & \frac{Y_{\delta r}}{u_0} \\ L_{\delta a} & L_{\delta r} \\ N_{\delta a} & N_{\delta r} \\ 0 & 0 \end{bmatrix} \begin{bmatrix} \Delta\delta_a \\ \Delta\delta_r \end{bmatrix} \quad (2)$$

The states for longitudinal motion are forward velocity (u),vertical velocity (w), pitch rate (q) and pitch angle (θ), and the control inputs are elevator (δ_e) and differential thrust (δ_T). For lateral motion, the states are sideslip angle (β), roll rate (p), yaw rate (r) and roll angle (ϕ), and the control inputs are aileron (δ_a) and rudder (δ_r).

Table 1. The nominal/undamaged aircraft data [4, 31, 32, 35, 40]

Flight Condition Properties	h (ft) = 40,000	I_x (slugs.ft^2)= 18.2×10^6
	M_∞= 0.9	I_y (slugs.ft^2)= 33.1×10^6
	α (degrees)= 2.4	I_z (slugs.ft^2)= 49.7×10^6
	W (lbf)= 636,636	V_∞(ft/s) = 871

Longitudinal		Lateral-directional	
Derivatives	Value	Derivative	Value
C_{Lo}	0.29	$C_{y\beta}$	-0.9
C_{Do}	0.0305	$C_{l\beta}$	-0.16
$C_{L\alpha}$	5.5	$C_{n\beta}$	0.16
$C_{D\alpha}$	0.5	C_{lp}	-0.34
$C_{m\alpha}$	-1.6	C_{np}	0.020
$C_{L\dot{\alpha}}$	8	C_{lr}	0.13
$C_{m\dot{\alpha}}$	-9.0	C_{nr}	-0.033
C_{Lq}	7.8	$C_{L\delta\alpha}$	0.014
C_{mq}	-25.5	$C_{n\delta\alpha}$	0.0018
C_{Lu}	-0.23	$C_{y\delta r}$	0.118
C_{Du}	0.22	$C_{l\delta r}$	0.008
C_{mu}	-0.09	$C_{n\delta r}$	-0.095
$C_{L\delta e}$	0.3	C_{yp}	0
$C_{m\delta e}$	-1.20	C_{yr}	0
$C_{x\delta e}$	0	-	-

3.2. Damaged aircraft models

3.2.1. Loss of 33% of left wing from tip. In a situation where an aircraft experiences a loss to some fraction of the wing, the mass and inertia properties will be greatly affected as a result of the change in C.G. position. “The new mass of the aircraft is determined based on empirical mass build-ups for similar aircraft and the wing CG is assumed to be at 40% of the mean aerodynamic chord and is set at half span. A mass build-up of the undamaged aircraft is adjusted to produce the same CG and inertia as the production aircraft. As tip portions of the left wing are removed or damaged the wing mass lowers and its CG shifts inboard. The aircraft CG then shifts positive along body centred Y axis and positive along the body centred X axis. Any shift along the Z axis is considered negligible” [3]. The stability derivatives will also be affected and, because the whole aerodynamic structure of the aircraft is affected, the new stability derivative values have to be calculated. Since the aircraft model in [3] was assumed to be a scaled model of the Boeing 747-200, the relationship between the mass property variations and the percentage wing loss of the aircraft had to be obtained in percentage. Doing so makes it possible to adapt the changes in mass and inertia properties for the aircraft model of this study.

The aerodynamic stability derivatives were however derived from [4], where the extended vortex lattice code Athena Vortex Lattice (AVL) was utilized to model and obtain the values of stability derivatives for undamaged and 33% left wing tip loss of a Generic Transport Model Aircraft (GTM). As [4] only had sufficient information for a 33% loss of the left wing from the tip, the same damage was adapted for this study. The generic transport model aircraft was again assumed to be a scaled model for the Boeing 747-200 aircraft as they both have similar aerodynamic structure. The difference in the aerodynamic stability derivatives for the undamaged and damaged model for the GTM was then obtained in terms of percentage (%). This percentage change was applied to the aircraft model for this study using the relationship: new stability derivative value for 33% wing damage = percentage change × initial stability derivative value

The values obtained and the percentage difference are summarised in Table 2. In case of an aircraft with a portion of the wing damaged, the damage causes coupling between the longitudinal and lateral

motion. It is important to note that, for this study, the effect of thrust was neglected for 33% loss of the left wing aircraft model. The linear equations of a wing damaged aircraft are [3]:

$$\begin{bmatrix} \Delta\dot{u} \\ \Delta\dot{\alpha} \\ \Delta\dot{q} \\ \Delta\dot{\theta} \\ \Delta\dot{\beta} \\ \Delta\dot{p} \\ \Delta\dot{r} \\ \Delta\dot{\phi} \end{bmatrix} = \begin{bmatrix} X_u & X_\alpha & X_q & -mgC_\theta & 0 & 0 & 0 & 0 \\ M_u & M_\alpha & (M_q - m\Delta xU) & mg(S_\theta\Delta x - C_\theta\Delta z) & 0 & 0 & 0 & 0 \\ Z_u & Z_\alpha & Z_q + mU & -mgS_\theta & 0 & 0 & 0 & 0 \\ 0 & 0 & 1 & 0 & 0 & 0 & 0 & 0 \\ 0 & 0 & 0 & 0 & Y_\beta & Y_p & Y_r - mu & mgC_\theta \\ 0 & 0 & m\Delta yU & -mgS_\theta\Delta y & L_\beta & L_p & L_r + m\Delta zU & -mgC_\theta\Delta z \\ 0 & 0 & 0 & mgC_\theta\Delta y & N_\beta & N_p & N_r - m\Delta xU & mgC_\theta\Delta x \\ 0 & 0 & 0 & 0 & 0 & 1 & \tan\theta & 0 \end{bmatrix} \begin{bmatrix} \Delta u \\ \Delta\alpha \\ \Delta q \\ \Delta\theta \\ \Delta\beta \\ \Delta p \\ \Delta r \\ \Delta\phi \end{bmatrix}$$

$$+ \begin{bmatrix} X_{\delta e} & 0 & 0 \\ M_{\delta e} & 0 & 0 \\ Z_{\delta e} & 0 & 0 \\ 0 & 0 & 0 \\ 0 & 0 & \frac{Y_{\delta r}}{u_0} \\ 0 & L_{\delta a} & L_{\delta r} \\ 0 & N_{\delta a} & N_{\delta r} \\ 0 & 0 & 0 \end{bmatrix} \begin{bmatrix} \Delta\delta_e \\ \Delta\delta_a \\ \Delta\delta_r \end{bmatrix} \quad (3)$$

Table 2. Flight conditions and stability derivatives for 33% left wing loss [3, 4]

Flight Condition Properties	h (ft)= 40,000		$\Delta x = 0.00$		
	M_∞= 0.9		Δy= 33090070		
	α (degrees)= 2.4		$\Delta z = 0$		
	W (lbf) = 623903.08		V_∞(ft/s) =871		
Mass properties					
Mass property	Δ%	New Value	Mass property	Δ%	New Value
Mass (slugs)	2	19391.53	I_x (slugs.ft^2)	17.5	15097500
b (ft)	17.7	161.06	$\bar{c}$ (ft)	-4.5	28.54
I_y(slugs.ft^2)	0.03	33090070	I_z(slugs.ft^2)	6.24	46598720
Stability Derivatives					
Derivatives	Δ%	New Value	Derivative	Δ%	New Value
C_{L0}	43.1	0.29588	$C_{y\beta}$	0.34	-0.89
C_{D0}	1.43	0.0443	$C_{l\beta}$	11.6	-0.141
$C_{m\alpha}$	25.3	-1.1952	$C_{n\beta}$	-0.32	0.1605
$C_{D\alpha}$	0	0.5	C_{lp}	32.6	-0.229
C_{mq}	1.2	-25.194	C_{np}	-14.2	-0.02284
$C_{L\alpha}$	13.7	4.75	C_{lr}	6.7	0.12
$C_{X\delta e}$	0	0	C_{nr}	0.05	-0.329
$C_{Z\delta e}$	0.67	0.29	$C_{L\delta\alpha}$	49.6	0.007056
$C_{m\delta e}$	0.08	-1.19	$C_{n\delta\alpha}$	0	0.0018
C_{yp}	8	0	$C_{y\delta r}$	0.02	0.117
$C_{n\delta r}$	0.05	-0.094	$C_{l\delta r}$	-0.3	0.008024

3.2.2. Complete loss of vertical stabilizer. To model the complete loss of the vertical stabilizer in this study, several simplifications were made such that the lateral-directional stability derivative had to be re-examined and recalculated. It is important to note that for most conventional civil transport aircraft, the vertical tail lies on the plane of symmetry. Knowing this allows for some assumptions so that the modelling process can be simplified. The loss of vertical stabilizer of an aircraft directly results in the

variation in values of some stability derivatives. The lateral-directional stability derivatives affected are [36]:

$$\{C_{y\beta}, C_{n\beta}, C_{l\beta}, C_{yp}, C_{np}, C_{lp}, C_{yr}, C_{nr}, C_{lr}\}$$

Denoting a variation in the values of the stability derivatives as Δ, one can write the unknown sets of derivative deviations as:

$$\{\Delta C_{y\beta}, \Delta C_{n\beta}, \Delta C_{l\beta}, \Delta C_{yp}, \Delta C_{np}, \Delta C_{lp}, \Delta C_{yr}, \Delta C_{nr}, \Delta C_{lr}\}$$

The relationship between the nominal values, variation and damaged values is given by:

$$\textit{New derivative value} = \textit{nominal value} - \textit{deviation value} \quad (4)$$

For the step-by-step derivation of this relationship as defined in Equation 4, please refer to [38]. The variation in some stability derivatives were obtained from [38], however, further factors had to be considered to obtain some of the other values. As a result of the complete loss of the vertical stabilizer, the vertical tail efficiency factor, volume and area will all be zero. Therefore, all stability derivatives that are dependent on these factors will be zero as well ($C_{y\beta} = C_{nr} = C_{yr} = 0$) [37]. In addition, vertical stabilizer is assumed to be primarily responsible for the weathercock stability of the aircraft, therefore bringing $C_{n\beta}$ to be equal zero as well ($C_{n\beta} = 0$) [37]. In addition, the mass and inertial properties of the aircraft will experience some changes but they are small compared to the change experienced in the wing loss scenario in the previous section [38]. The mass and inertia properties in Table 3 reflect the complete loss of the vertical stabilizer scenario. All values used for the stability derivatives deviation are summarised in Table 4. The stability derivative values used for the modelling of complete loss of vertical stabilizer for the Boeing 747-200 in this study are given in Table 5.

Table 3. Complete loss of vertical stabilizer mass and inertia data [38]

Parameter	Value
W (lbf)	629540
m (slugs)	19566.10
I_x (slugs.ft^2)	17893000
I_y (slugs.ft^2)	30925000
I_z (slugs.ft^2)	47352000

Table 4. Deviation values for complete loss of vertical stabilizer [37, 38]

Vertical Tail Contributions to Lateral-Directional Derivatives Variation		
$\Delta C_{y\beta}^{(max)} = -0.451$	$\Delta C_{l\beta}^{(max)} = -0.068$	$\Delta C_{n\beta}^{(max)} = 0.234$
$\Delta C_{yp}^{(max)} = -0.137$	$\Delta C_{lp}^{(max)} = -0.021$	$\Delta C_{np}^{(max)} = 0.071$
$\Delta C_{yr}^{(max)} = 0.467$	$\Delta C_{lr}^{(max)} = 0.071$	$\Delta C_{nr}^{(max)} = -0.242$

Table 5. Stability derivatives for complete loss of vertical stabilizer

Lateral-Directional Stability Derivatives After Complete loss of Vertical tail		
$C_{y\beta} = 0$	$C_{l\beta} = -0.092$	$C_{n\beta} = 0$
$C_{yp} = -0.137$	$C_{lp} = -0.319$	$C_{np} = -0.091$
$C_{yr} = 0$	$C_{lr} = 0.059$	$C_{nr} = 0$
Lateral-Directional Control Derivatives After Complete loss of Vertical tail		
$C_{y\delta\alpha} = 0$	$C_{l\delta\alpha} = 0.014$	$C_{n\delta\alpha} = 0.0018$
$C_{y\delta r} = 0.118$	$C_{l\delta r} = 0.008$	$C_{n\delta r} = -0.095$

For an aircraft with complete loss of vertical stabilizer, the differential thrust component (δ_T) will be used as the alternate control input since the rudder has been lost due to the damage. The lateral directional state space equation for an aircraft with complete loss of vertical stabilizer is given by [37]:

$$\begin{bmatrix}\Delta\dot{\beta}\\ \Delta\dot{p}\\ \Delta\dot{r}\\ \Delta\dot{\phi}\end{bmatrix}=\begin{bmatrix}\frac{Y_\beta}{u_0} & \frac{Y_p}{u_0} & -\left(1-\frac{Y_r}{u_0}\right) & \frac{g\cos\theta_0}{u_0}\\ L_\beta & L_p & L_r & 0\\ N_\beta & N_p & N_r & 0\\ 0 & 1 & 0 & 0\end{bmatrix}\begin{bmatrix}\Delta\beta\\ \Delta p\\ \Delta r\\ \Delta\phi\end{bmatrix}+\begin{bmatrix}0 & 0\\ L_{\delta a} & \frac{\bar{I}_{xz}y_e}{\bar{I}_x\bar{I}_z-\bar{I}_{xz}^2}\\ N_{\delta a} & \frac{\bar{I}_x y_e}{\bar{I}_x\bar{I}_z-\bar{I}_{xz}^2}\\ 0 & 0\end{bmatrix}\begin{bmatrix}\Delta\delta_a\\ \Delta\delta_T\end{bmatrix} \quad (5)$$

4. Plant dynamics

4.1. Undamaged aircraft plant dynamics

The equations presented below represent the state space matrices for nominal flight condition. The matrices Alo_n and Blo_n are for longitudinal motion whereas matrices Ala_n and Bla_n are for lateral-directional motion. *C* and *D* matrices for both longitudinal and lateral motion are identity matrix and zero matrix respectively.

$$Alo_n=\begin{bmatrix}-0.02204 & 0.001422 & 0 & -32.17\\ -0.05759 & -0.3943 & 871 & 0\\ -0.000095 & -0.001793 & -0.5468 & 0\\ 0 & 0 & 1 & 0\end{bmatrix},\ Blo_n=\begin{bmatrix}0 & 0.0000191\\ -18.58 & 0\\ -1.2 & 0\\ 0 & 0\end{bmatrix} \quad (6)$$

$$Ala_n=\begin{bmatrix}-0.06399 & 0 & -1 & 0.03691\\ -2.111 & -0.5048 & 0.193 & 0\\ 0.7732 & 0.01087 & -0.1794 & 0\\ 0 & 1 & 0 & 0\end{bmatrix},\ Bla_n=\begin{bmatrix}0 & 0.00839\\ 0.1\,848 & 0.1056\\ -0.008699 & -0.4591\\ 0 & 0\end{bmatrix} \quad (7)$$

The damping characteristics for the longitudinal motion of the undamaged aircraft are given in Table 6. The results show two conjugate complex pairs of eigenvalues with negative real parts. The step input plot is shown in Figure 1 and it can be clearly seen from this plot that the system becomes stable after a while for all states and inputs. The eigenvalues and modes for the lateral-directional motion of the undamaged aircraft are shown in Table 7. Since all real parts of the eigenvalues are negative, the open loop system is stable [30]. The open loop system's response to a step input for lateral motion is shown in Figure 2 and, as in the case of the longitudinal motion, the system tends towards being stable after some time.

Table 6. Longitudinal motion characteristics for undamaged aircraft

Eigenvalue/pole location	Damping Ratio (ζ)	Frequency (ω)	Mode
-0.472 + 1.25i	0.354	1.33	Short period
-0.472 - 1.25i	0.354	1.33	Short period
-0.00988+ 0.0331i	0.287	0.0345	Phugoid
-0.00988 - 0.0331i	0.287	0.0345	Phugoid

Table 7. Lateral/directional motion characteristics for undamaged aircraft

Eigenvalue	Damping Ratio (ζ)	Time Constant (s)	Frequency (ω)	Mode
-0.0698 + 0.9i	0.0773	-	0.890	Dutch roll
-0.0698 - 0.9i	0.0773	-	0.890	Dutch roll
-0.591	-	1.69	0.547	Roll
-0.0176	-	56.8	0.0195	Spiral

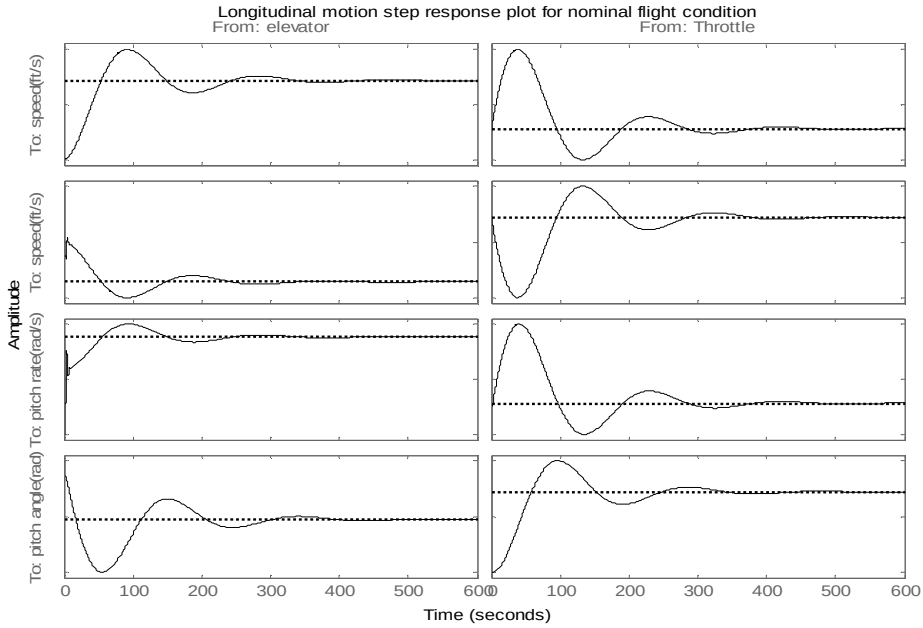

Figure 1. Step response plot for longitudinal motion for nominal flight condition

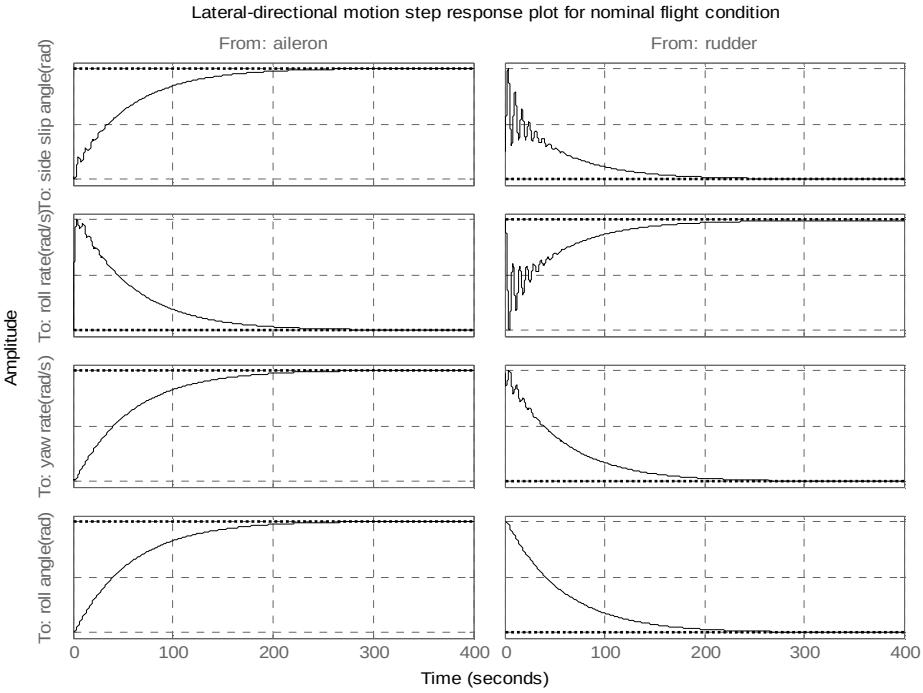

Figure 2. Step response plot for lateral/ directional motion for nominal flight condition

4.2. Damaged aircraft plant dynamics

4.2.1. Loss of 33% of left wing from tip. The first damage scenario is presented in this section. The following equations presented represent the state space matrices after the model aircraft experiences a 33% loss of the left wing from the tip. The subscript '*wd*' is to indicate that damage has been done to part of the wing.

$$A_{wd}=\begin{bmatrix} -0.0047 & -0.01077 & 0 & -623300 & 0 & 0 & 0 & 0 \\ -0.31 & -0.253 & 1.678e+7 & -28300 & 0 & 0 & 0 & 0 \\ 0 & 0 & -1.579e+5 & 264.6 & 0 & 0 & 0 & 0 \\ 0 & 0 & 1 & 0 & 0 & 0 & 0 & 0 \\ 0 & 0 & 0 & 0 & -0.047 & 0 & -1.689e+7 & 6.2e+5 \\ 0 & 0 & 4653000 & -7797 & -0.0016 & -0.2013 & 0.1055 & 0 \\ 0 & 0 & 0 & 171900 & 0.00057 & -0.0065 & -157900 & 5833 \\ 0 & 0 & 0 & 0 & 0 & 1 & 0.04541 & 0 \end{bmatrix}$$

$$B_{wd}=\begin{bmatrix} 0 & 0 & 0 \\ 13.33 & 0 & 0 \\ -0.9147 & 0 & 0 \\ 0 & 0 & 0 \\ 0 & 0 & 5.377 \\ 0 & 0.06708 & 0.07629 \\ 0 & 13.32 & -0.2895 \\ 0 & 0 & 0 \end{bmatrix} \quad (8)$$

The eigenvalues of all modes for damaged and wing damaged aircraft systems are shown in Table 8 for comparison. One of the eigenvalues for 33% left wing damage has a positive real part and for this reason, the overall system is unstable. Other damping characteristics for the undamaged and the wing damaged aircraft models are shown in Table 9.

Table 8. Eigenvalues for undamaged and wing-damaged aircraft model

Category	Mode	Undamaged	33% damage
Longitudinal	Long period	-0.00988 + 0.0331i -0.00988 - 0.0331i	-0.602 + 0.861i -0.602 - 0.861i
	Short period	-0.472 +1.25i -0.472 - 1.25i	**-15800** **-15800**
Lateral	Roll	-0.591	**0.896**
	Spiral	-0.017	-0.367
	Dutch roll	-0.0698 + 0.9i -0.0698 - 0.9i	-0.000547+ 0.0186i -0.000547- 0.0186i

Table 9. Other characteristics for undamaged and wing-damaged aircraft model

Category	Mode	Undamaged			33% damage		
		ζd	*ωd (rad/s)*	*Time constant (s)*	*ζd*	*ωd (rad/s)*	*Time constant (s)*
Longitudinal	Long period	0.287 0.287	0.0345 0.0345	- -	0.573 0.573	1.05 1.05	- -
	Short period	0.354 0.354	1.33 1.33	- -	- -	158000 158000	0.00000633 0.00000633
Lateral	Roll	-	0.591	1.69	-	0.896	1.12
	Spiral	-	0.0176	56.8	-	0.367	2.73
	Dutch roll	0.0773 0.0773	0.902 0.902	- -	0.0293 0.0293	0.0187 0.0187	- -

The system for wing damaged aircraft turned out to not be controllable and observable. Therefore, a control system was not designed for this scenario. Observability and controllability of a system will be further explained in later section 5.

With all the derivations and equations involved in modeling a wing damaged aircraft, it is very important to validate the results obtained. Due to the lack of published information in this area of focus for this particular aircraft, other measures of validation needed to be taken. A similar study was carried out by [3] on how a 33% loss of the left wing affects the stability of a GTM aircraft. An analysis regarding the stability of the aircraft after damage was carried out. It was found that at a velocity of 160ft/s and an altitude of 625ft, the aircraft was only able to trim up to about 26% damage. It was also stated in this study that it was of a great concern that the aircraft would be unable to trim at higher damage, higher altitude and higher velocity [3]. From the results obtained, after experiencing a 33% loss of the left wing, the aircraft system was not controllable and observable. Hence a controller could not be implemented to make the system stable. This is a reasonably valid result. This could be due to the ailerons' inability to overcome the rolling moment caused by the damage. Also stated in study from [3] was that the effect of this type of damage will be greater on the roll and short period modes. A similar conclusion was reached from the results obtained in this study as the most affected modes were the short period and roll mode. The effect it has on the roll mode is due to the fact that roll mode eigenvalue is dominated by C_{lp}, which is reduced by damage [3]. Although the effects are not of exact same magnitude, this could be due to some kind of error caused by some of the assumptions made. In addition, uncontrollability of the system could be due to the fact that the effect of thrust was neglected during the modelling process because using the differential thrust from the engines in a situation like this, the aircraft is usually able to stabilise itself after suffering 33% loss of its left wing [39].

4.2.2. Complete loss of vertical stabilizer. The second damage scenario is presented in this section. The equations presented below represent the state space matrices after experiencing complete loss of the vertical stabilizer. '*vsd*' is used to indicate that damage has been done to the vertical stabilizer.

$$A_{vsd}=\begin{bmatrix} 0 & -0.001108 & -1 & 0.03691 \\ -1.235 & -0.4818 & 0.08911 & 0 \\ 0 & -0.05193 & 0 & 0 \\ 0 & 1 & 0 & 0 \end{bmatrix}$$
$$B_{vsd}=\begin{bmatrix} 0 & 0 \\ 0.1879 & 0.0142 \\ 0 & 0.6801 \\ 0 & 0 \end{bmatrix} \quad (9)$$

The open loop system response analysis was carried out on the damaged aircraft. The eigenvalues are shown in Table 10 and it clearly indicates the unstable nature of the Dutch roll mode as the real parts are positive. In addition, the pole location of the spiral mode is at the origin, which represents a very slow to unstable dynamics. The roll mode is the only stable mode of vertical-stabilizer-damaged aircraft as the eigenvalue for this mode has a negative real part (**-0.7**). The open loop step response plot in Figure 3 shows the divergent nature of the system implies that the system is unstable. Unlike the first scenario addressed, this system is observable and also controllable.

Table 10. Damping characteristics of the damaged aircraft (complete loss of vertical stabilizer)

Eigenvalue	Damping Ratio (ζ)	Time Constant(s)	Frequency (ω)	Mode
0.109 + 0.38i	-0.277	-	0.396	Dutch roll
0.109- 0.38i	-0.277	-	0.396	Dutch roll
-0.7	-	1.43	0.7	Roll
0	-	-	-	Spiral

For validation purposes, in the case of the complete loss of the vertical stabilizer of the aircraft model used in this study, a similar research was carried out on the same aircraft model but for different flight condition in [37]. The spiral and Dutch roll mode became unstable after damage. Similar results

were achieved in this study as spiral and Dutch roll mode became unstable after the complete loss of the aircraft's vertical stabilizer.

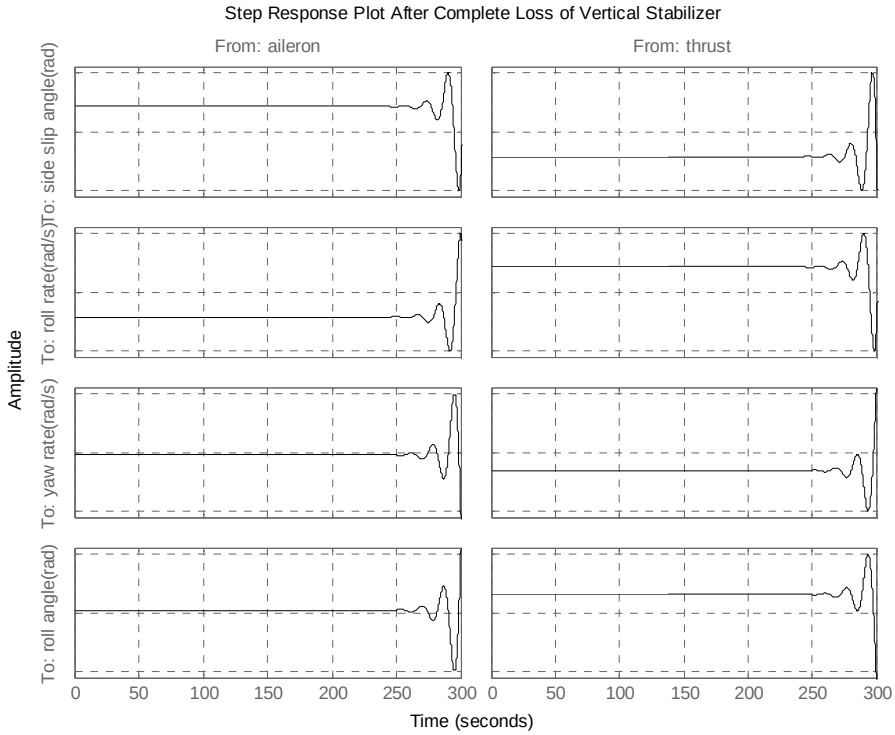

Figure 3. Step response plot for complete loss of vertical stabilizer

5. Linear Quadratic Regulator (LQR) design for controllable and observable damaged aircraft model

5.1. Controllability and observability

Controllability and observability are two very important characteristics of any system. Controllability determines the possibility of achieving the desired system states response using the input. To check the controllability of a system, the matrix given in Equation 10 is used. If the matrix is full rank, then the system is controllable [30]. Observability, on the other hand, is to know the possibility of determining all the states from the output and input signals. The system is observable if the matrix in Equation 11 is full rank. MATLAB functions *ctrb(A,B)* and *obsv(A,C)* gives the controllability matrix, $\boldsymbol{V}$ and also observability matrix, $\boldsymbol{O}$ respectively.

$$\boldsymbol{V} = [B, AB, A^2B, \ldots, A^{n-1}B] \tag{10}$$

$$\boldsymbol{O} = [C^T, A^TC^T, \ldots, (A^T)^{n-1}C^T] \tag{11}$$

where n is the order of the vector $\underline{x}$ in the state space representation.

The rank of the controllability and observability matrices for 33% loss of left wing does not equal to $n((rank(V)\neq n\neq 8),(rank(O)\neq n\neq 8))$. This means that the system is not controllable or observable and due to this, the LQR controller was implemented for this damage scenario. On the other hand, after introducing the complete loss of the vertical stabilizer for the aircraft model, the system still remained controllable and observable for this case. This means the rank of the controllability and observability matrices for this damage scenario was equal to $n((rank(V)=n=4),(rank(O)=n=4))$. Hence, a full state feedback LQR controller was implemented to return the aircraft to stable condition.

5.2. Background on LQR control

Optimal control aims at producing the best results using minimum control efforts for a given set of constraints. Basically, the ultimate objective of an optimal controller is to find optimal feedback gain that can fulfil a certain performance index (PI) given a certain condition. A type of optimal controller which is the LQR is presented below. An optimal regulator problem taken from [33] is considered.

Given the equation of a system: $\dot{x}=Ax+Bu$ (12)

Determine K of the optimal vector: $u=-Kx$ (13)

Such that it minimizes the performance index: $J=\int_0^{\infty}(x^TQx+u^TRu)dt$ (14)

where Q and R are real and positive definite symmetric matrices. Q acts as a weighing matrix while R acts as the control cost matrix.

$$K=T^{-1}(T^T)^{-1}B^TP=R^{-1}B^TP \tag{15}$$

P is called a Riccati matrix and is found by solving the Riccati equation:

$$A^TP+PA-PBR^{-1}B^TP+Q=0 \tag{16}$$

MATLAB '*lqr(A,B,Q, R)*' function solves the Algebraic Ricatti Equation (ARE) and finds optimal gain '*K*' matrix. However, the dilemma of choosing the magnitude of the state weighing matrix Q and the control cost matrix R still lingers. A very simple method widely used to choose the matrices Q and R is given by Bryon's rule [34]. These matrices are selected with:

$$Q_{ii}=\frac{1}{\text{maximum acceptable value of } z_i^2} \qquad i\in\{1,2,\ldots,k\} \tag{17}$$

$$R_{jj}=\frac{1}{\text{maximum acceptable value of } u_j^2} \qquad j\in\{1,2,\ldots,k\} \tag{18}$$

Simply put, what Bryson's rule does is to scale the variables in J_{LQR} such that the maximum value is acceptable is one for each term [34]. Doing this is of great essence because, for example, if the unit of each variable differs, the full range possible for each state will also differ. So a way to normalize them is by thinking about the full range that each state can take and choosing initial guesses. The Bryson's rule usually marks the starting point for an iterative process in order to obtain the desired performance for a closed loop system [34].

5.3. Stabilizing damaged aircraft with LQR controller

After an iterative process, the magnitude of matrix Q and R chosen are shown in Equations 19 and 20. respectively. The gain '*K*' matrix found was then used in the SIMULINK model. The feedback matrix K obtained is shown in Equation 22. Figure 4 represents the block diagram used for the full state feedback LQR control system design using SIMULINK.

$$Q=50000\begin{bmatrix}1&0&0&0\\0&1&0&0\\0&0&1&0\\0&0&0&1\end{bmatrix} \tag{19}$$

$$R=\begin{bmatrix}1&0\\0&1\end{bmatrix} \tag{20}$$

$$K_{LQR}=\begin{bmatrix}1.4409 & 226.2909 & -3.6333 & 223.7670\\ -223.5598 & 3.9505 & 225.0357 & -0.2905\end{bmatrix} \tag{21}$$

Equation 22 represents the new A matrix after implementing an LQR controller into the system. '*LQR*' is used to indicate the implementation of LQR controller.

$$A_{LQR}=\begin{bmatrix} 0 & -0.001108 & -1 & 0.03691 \\ 1.669 & -43.06 & -2.424 & -42.05 \\ 152 & -2.739 & -153.1 & 0.1976 \\ 0 & 1 & 0 & 0 \end{bmatrix} \quad (22)$$

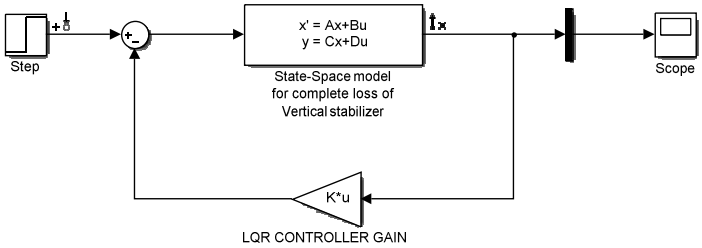

Figure 4. Block diagram used for the full state feedback LQR control system design

The new eigenvalues of the system before and after implementing the LQR controller are shown in Table 11. Using the eigenvalues, the system returns to being stable after implementation of the LQR system (all eigenvalues have negative real parts). The other damping characteristics for undamaged, vertical stabilizer damaged and LQR controlled systems are also shown in Table 12 for comparison purposes. The closed loop/feedback step response plot of the system after control is shown in Figure 5. The response plot also confirms that with the use of an LQR controller the system becomes stable in all four states after a period of time.

For validation, in reference [37], a LQR controller was also implemented for the same aircraft that suffered the same damage but for a different flight condition (lower altitude) and found to successfully stabilize all four states of the aircraft within 15 seconds. Using a Linear Quadratic Regulator (LQR) controller in this study has also yielded a similar result as the controller stabilized the damaged aircraft within 6 seconds.

Table 11. Comparison of eigenvalues for the undamaged, complete loss of vertical stabilizer and LQR controlled system

Category	Mode	Undamaged	Complete loss of vertical stabilizer	LQR controlled system
Lateral	Roll	-0.591	-0.7	-42
	Spiral	-0.0176	0	-152
	Dutch roll	-0.0698+ 0.9i	0.109 + 0.38i	-1 +0.0186
		-0.0698 - 0.9i	0.109 - 0.38i	-1 – 0.0186

Table 12. Other damping characteristics for the undamaged, vertical stabilizer damaged and LQR controlled system

Mode	Undamaged			Complete loss of vertical stabilizer			LQR controlled system		
	ζd	*ωd (rad/s)*	*Time constant (s)*	*ζd*	*ωd (rad/s)*	*Time constant (s)*	*ζd*	*ωd (rad/s)*	*Time constant (s)*
Roll	-	0.591	1.69	-	0.701	1.43	-	42	0.0238
Spiral	-	0.0176	56.8	-	0	-	-	152	0.00657
Dutch	0.0773	0.902	-	0.277	0.396	-	1	1	-
roll	0.0773	0.902	-	0.277	0.396	-	1	1	-

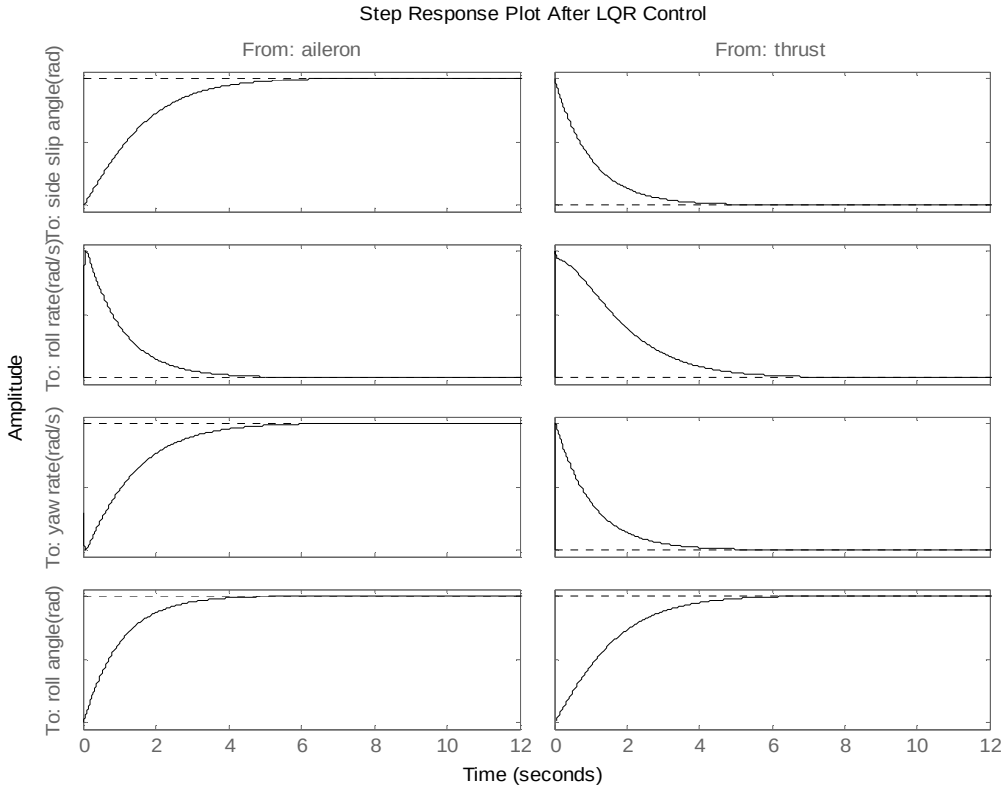

Figure 5. Step response plot after LQR controller

Finally, to know the true performance of the LQR controller, the time response characteristics (rise time, settling time, percentage overshoot) for undamaged and LQR controlled systems were compared. Table 13 shows the response characteristics due to input one (aileron) whereas Table 14 shows the response characteristics due to the second input (differential thrust). After the implementation of the LQR controller as a result of damage, the performance of the system has improved compared to its performance in nominal condition for all state variables. The controller can obviously stabilize the system within only 6 seconds, unlike the undamaged aircraft which stabilizes within 230 seconds.

Table 13. Time response characteristics due to aileron

State variable	Undamaged			LQR controlled system		
	Rise time(s)	*Settling time(s)*	Percentage Overshoot	*Rise time(s)*	*Settling time(s)*	Percentage Overshoot
Sideslip angle (β)	125	219	0	3.09	5.25	0
Roll rate (p)	0	228	-	12	4.03	0
Yaw rate (r)	125	224	0	2.76	4.97	0
Roll angle (ϕ)	125	224	0	2.2	3.94	0

Table 14. Time response characteristics due to differential thrust

State variable	Undamaged			LQR controlled system		
	Rise time(s)	*Settling time(s)*	Percentage Overshoot	*Rise time(s)*	*Settling time(s)*	Percentage Overshoot
Sideslip angle (β)	125	200	0	2.2	3.91	0
Roll rate (p)	0	207	-	-	5.81	-
Yaw rate (r)	131	222	0	-	3.97	-
Roll angle (ϕ)	125	224	0	3.09	5.21	0

6. Conclusion

The area of focus of this work is to model the dynamics of a damaged Boeing 747-200 aircraft and to implement a control system to the observable and controllable damaged system to regain the stability of the damaged aircraft. The stability derivatives for undamaged aircraft were obtained. Two damage scenarios were considered and in both cases, the stability derivative values experienced some changes and had to be re-examined and recalculated. The modelling of the 33% loss of the left wing showed that the system was not controllable or observable. On the other hand, for the complete loss of the vertical stabilizer, the system proved to be controllable and also observable. Simulations were also used to show the aircraft's response to damages. A LQR controller was implemented to return the aircraft to trim condition. The LQR controller was proven to be able to make the aircraft stable and also improve the performance characteristics.

References

[1] Romanucci and Blandin *5 Most Common Causes of Plane Crashes*
[2] Fielding C and Luckner R 2000 *IEE Control Engineering Series* 1-55
[3] Arruda M 2009 *Dynamic inverse resilient control for damaged asymmetric aircraft: Modeling and simulation* Doctoral dissertation Wichita State University
[4] Ouellette J, Raghavan B, Patil M J and Kapania R K 2009 *AIAA Atmospheric Flight Mechanics Conference* p. 6153
[5] Jordan T, Langford W, Belcastro C, Foster J, Shah G, Howland G and Kidd R 2004 *AUVSI's Unmanned Systems North America Symposium and Exhibition*
[6] Jordan T L, Langford W M and Hill J S 2005 *AIAA Guidance, Navigation and Control Conference and Exhibit*
[7] Beltramo M N, Trapp D L, Kimoto B W and Marsh D P 1977 *Parametric study of transport aircraft systems cost and weight*
[8] Woo J H 1992 *AIAA/USAF/NASA/OAI Symposium on Multidisciplinary Analysis and Optimization*
[9] Render P M, Samaad-Suhaeb M, Yang Z and Mani M 2009 *Journal of Aircraft*, **46** 997-1004
[10] Foster J V, Cunningham K, Fremaux C M, Shah G H, Stewart E C, Rivers R A, Wilborn J E and Gato W 2005 *AIAA Paper*
[11] Shah G H 2008 *AIAA Atmospheric Flight Mechanics Conference and Exhibit*
[12] Thomas A L 1993 *Proceedings of the Royal Society of London B: Biological Sciences* **254** 181-9

[13] Keller J D, McKillip Jr. R M and Wachspress D A 2008 *AIAA Paper*
[14] Wilborn J E and Foster J V 2004 *AIAA atmospheric flight mechanics conference and exhibit*
[15] Bacon B J and Gregory I M 2007 *General equations of motion for a damaged asymmetric aircraft*. American Institute of Aeronautics and Astronautics
[16] Nguyen N, Krishnakumar K, Kaneshige J and Nespeca P 2006 *AIAA Guidance, Navigation, and Control Conference and Exhibits*
[17] Nguyen N T, Krishnakumar K S, Kaneshige J T and Nespeca P P 2008 *Journal of Guidance, Control and Dynamics* **31** 751-64
[18] Nguyen N T, Krishnakumar K S, Kaneshige J T and Nespeca P P 2008 *Journal of Guidance, Control and Dynamics* **31** 751-764
[19] Liu Y, Tao G and Joshi S M 2010 *Journal of Guidance, Control and Dynamics* **33** 1500-17
[20] Lee S and Sharma M 1998 *Direct adaptive reconfigurable control of a tailless fighter aircraft*
[21] Nguyen N T, Bakhtiari-Nejad M and Huang Y 2007 *AIAA Guidance, Navigation and Control Conference and Exhibit*
[22] Kim B S and Calise A J 1997 *Journal of Guidance, Control and Dynamics* **20** 26-33
[23] Rysdyk R T and Calise A J 1999 *Journal of Guidance, Control and Dynamics* **22** 402-7
[24] Shin Y, Calise A J and Johnson M 2008 *Journal of Guidance, Control and Dynamics* **31** 1464-77
[25] Burcham Jr F W, Maine T A, Fullerton C G and Webb L D 1996 *Development and flight evaluation of an emergency digital flight control system using only engine thrust on an F-15 airplane*
[26] Burcham F W, Maine T A and Burken J J 1996 *Development and flight test of an augmented thrust-only flight control system on an MD-11 transport airplane* National Aeronautics and Space Administration
[27] Bull J, Mah R, Hardy G, Sullivan B, Jones J, Williams D, Soukup P and Winters J 1997 *Piloted simulation tests of propulsion control as backup to loss of primary flight controls for a B747-400 jet transport*
[28] Johnson E N, Calise A J and Blauwe H D 2008 *AIAA Guidance, Navigation and Control Conference*
[29] Tang Y, Atkins E and Sanner R 2007 *AIAA Guidance, Navigation and Control Conference and Exhibit*
[30] Nelson R C 1998 *Flight stability and automatic control* (New York: McGraw Hill)
[31] Caughey D A 2011 *Introduction to aircraft stability and control course notes for M&AE 5070* Cornell University
[32] Napolitano M R 2012 *Aircraft dynamics: From modeling to simulation (*Wiley)
[33] Ogata K and Yang Y 1970 *Modern control engineering*
[34] Hespanha J 2005. *Lecture notes on lqr/lqg controller design*
[35] Roskam J 2006 *Airplane Design: Part I-VIII* (Lawrence: DARcorporation)
[36] Bramesfeld G, Maughmer M D and Willits S M 2006 *Journal of aircraft* **43** 216-25
[37] Lu L 2015 *Utilization of Differential Thrust for Lateral/Directional Stability of a Commercial Aircraft with a Damaged Vertical Stabilizer*
[38] Hitachi Y 2009 *Damage-Tolerant Flight Control System Design for Propulsion-Controlled Aircraft* Doctoral dissertation University of Toronto
[39] Sarigul-Klijn N, Rapetti R, Jordan A, Lopez I, Sarigul-Klijn M and Nespeca P 2010 *Journal of Aircraft* **47** 255-67
[40] Lu L and Turkoglu K 2015 *Adaptive Differential Thrust Methodology for Lateral/Directional Stability of an Aircraft with a Damaged Vertical Stabilizer*